Rate constants in quantum mechanical systems: A rigorous and practical path-integral formulation for computer simulations

Nilmadhab Chakrabarti, Tucker Carrington Jr., Benoît Roux

Départements de physique et de chimie, Université de Montréal, C.P. 6128, succursale Centre-Ville, Montréal (Québec), H3C 3J7 Canada

Abstract

In this letter we present rigorous equations, amenable to computer simulations, for using Feynman path integrals to calculate thermal rate constants. The quantum mechanical expression for the thermal rate constant in terms of the derivative of a side–side correlation function developed by Miller, Schwartz and Tromp (J. Chem. Phys. 79 (1983) 4889) is used. We calculate the side–side correlation function with a discretized Feynman path integral. The derivative of the side–side correlation function is calculated using statistical mechanical free energy perturbation calculation methods *after* computing the trace. The theory is illustrated with the Monte Carlo simulation of a free particle. © 1998 Elsevier Science B.V. All rights reserved.

1. Introduction

The laws of classical mechanics have been used to calculate rate constants for several decades. Rate constants were first computed for simple atom–diatom exchange reactions [1] but essentially the same ideas are used today to compute rate constants for very complex molecular processes. Classically, one computes a thermal rate constant from a correlation function obtained by solving Newton's equations of motion in a small region of the potential energy surface close to the dividing surface which distinguishes reactants from products [2–8].

For many reactions a classical calculation is perfectly adequate, but for some processes quantum effects are important. In general, quantum effects are important at low temperatures and for reactions which involve the exchange of light nuclei. In particular, quantum effects are often significant in proton transfer reactions. Although such processes have always received special attention due both to their practical importance and to their special properties, there exists no practical computational treatment for complex systems for which quantum effects are important. In this letter we present a rigorous quantum mechanical method for calculating thermal rate constants via computer simulations. Exact quantum mechanical equations which enable one to calculate a rate constant were derived several years ago by Yamamoto [9], Miller [10], and Miller, Schwartz and Tromp (MST) [11]. Several approaches for using the MST and Yamamoto equations have been devised and applied. They can be divided into two groups: (1) those which require the storage of vectors which represent wavefunctions in some basis set [12–16]; (2) those which use discretized Feynman path integral simulations [17–19]. Theories constructed around the concept of the path centroid have been developed by Gillan [17] and

by Voth, Chandler and Miller [18,19]. Voth, Chandler and Miller (VCM) have shown that the exact rate constant may be related to the Kubo transform of a flux–flux time correlation function. However, their formulation involves real-time propagators which are not easily calculated by computer simulations. Here we describe a closely-related approach based on Feynman path integrals [20–22]. Our method is both rigorous (it is derived from first principles) and amenable to computer simulations (our final equation for the rate constant is written in terms of computable averages). In contrast to VCM, the formulation we present in this Letter involves real distributions which can be sampled in computer simulations. The theoretical formulation and computational details are given in Section 2. The relationship with transition state theory (TST) is discussed and the method is illustrated in Section 3. The Letter is briefly concluded in Section 4.

2. Theory and method

In this section we present equations for calculating thermal rate constants. Formal equations for the thermal rate constant of a chemical reaction are well-known but a good practical scheme for evaluating rate constants is lacking. Because we wish to develop a scheme applicable to multidimensional problems (for which the dimensionality of configuration space is too large to permit storing a basis representation of a wavefunction) we employ Feynman path integrals [20]. We use Cartesian coordinates because path integrals are much easier in Cartesian coordinates. In Cartesian coordinates a quantum system of N atoms is described by the Hamiltonian $H = T + V$,

$$H = \sum_{i=1}^{N} \frac{1}{2m_i} P_i^2 + V(x) \tag{1}$$

where m_i is the mass of the i-th atom and $x \equiv \{x^{(1)}, x^{(2)}, \ldots, x^{(N)}\}$ represents all $3N$ Cartesian coordinates. Our goal is to calculate the rate constant for the transitions between two regions, a and b, of multi-dimensional configurational space. There may be a high barrier between regions a and b. In this case the transition is called an activated process because it occurs only if the reacting particles have the necessary activation energy. If the probability that the reactants have enough energy to cross the barrier is small, the reaction is a rare event [4]. Rate constants are difficult to calculate when the probability of crossing the barrier is small.

To calculate a rate constant one defines a dividing surface which distinguishes between regions a and b. Points on one side of the dividing surface are in region a; points on the other side are in region b. It is customary to construct a dividing surface by using a reaction coordinate function. For example, one may choose the function $q[x]$ such that $q[x] < 0$ if the point x is in region a and $q[x] > 0$ if the point x is in region b. In a classical treatment, one calculates a thermal rate constant from the classical flux through the dividing surface. To compute the flux through the dividing surface it is necessary to solve classical equations of motion only in a small region of configuration space close to the dividing surface. It is therefore much easier to calculate classical rate constants than quasi-classical state-to-state transition probabilities. Miller, Schwartz and Tromp (MST) [11] have developed equations which allow one to calculate, using quantum mechanics, rate constants more easily than state-to-state detailed information. MST present equations for the forward rate constant in terms of either a side–side, a flux–side or a flux–flux correlation function. For our purposes the formulation in terms of the side–side correlation function is the most useful. According to the MST formulation [11], the forward rate constant is

$$Q_a k = \lim_{t \to \tau_m} \dot{C}_s(t) \tag{2}$$

where $\dot{C}_s(t)$ is the time derivative of a side–side correlation function; Q_a is the partition function (per unit volume) of region a

$$Q_a = \mathrm{tr}\left[e^{-\beta H} h_a \right] \tag{3}$$

and τ_{m} is a time long compared to the rapid dynamics occurring near the barrier top, but nevertheless much smaller than $1/k$, the characteristic relaxation time in a two-state bound system [2,23]. For unbound systems this relaxation does not occur. The a–b (left–right) side–side correlation function is,

$$C_s(t) = \mathrm{tr}\left[h_a \mathrm{e}^{+i\tau^* H/\hbar} h_b \mathrm{e}^{-i\tau H/\hbar} \right] \tag{4}$$

where $\tau = t - i\beta\hbar/2$ is a complex time, $\beta = 1/k_B T$ and h_a and h_b are the population operators corresponding to regions a and b respectively. This correlation function is symmetrized with respect to the propagators on both sides of the operator h_b. It can be shown that $C_s(t)$ is real.

It is difficult to use the MST equation to calculate the rate constant at a given temperature because of the real-time evolution operator. To evaluate the trace in Eq. (4) we use a path-integral approach. To use path integrals one needs to compute averages in a multidimensional space. Whenever the integrand can be written as a product of a positive definite weight function and a smooth well-behaved function, a multidimensional integral can be computed with an importance sampling algorithm. Computing the trace in Eq. (4) is, however, not straightforward because it involves real-time propagators and the integrand is not written as a product of a positive weight function and a smooth function. If we write the rate constant as

$$k = \lim_{t \to \tau_{\mathrm{m}}} \frac{Q}{Q_a} \dot{G}_s(t) \tag{5}$$

where Q is the partition function

$$Q = \mathrm{tr}\left[\mathrm{e}^{-\beta H} \right] \tag{6}$$

and

$$G_s(t) = \frac{1}{Q} \mathrm{tr}\left[h_a \mathrm{e}^{+i\tau^* H/\hbar} h_b \mathrm{e}^{-i\tau H/\hbar} \right] \tag{7}$$

we can apply ideas developed by Thirumalai and Berne [24] for calculating complex-time path integrals to compute the rate constant. Note that Q_a/Q is the probability of the system being in region a. By evaluating both the numerator and the denominator of $G_s(t)$ in the coordinate representation we obtain

$$G_s(t) = \frac{\int d\boldsymbol{x}_1 d\boldsymbol{x}_{P+1} h_a(q[\boldsymbol{x}_1]) h_b(q[\boldsymbol{x}_{P+1}]) \langle \boldsymbol{x}_1 | \mathrm{e}^{+i\tau^* H/\hbar} | \boldsymbol{x}_{P+1} \rangle \langle \boldsymbol{x}_{P+1} | \mathrm{e}^{-i\tau H/\hbar} | \boldsymbol{x}_1 \rangle}{\int d\boldsymbol{x}_1 d\boldsymbol{x}_{P+1} \langle \boldsymbol{x}_1 | \mathrm{e}^{+i\tau^* H/\hbar} | \boldsymbol{x}_{P+1} \rangle \langle \boldsymbol{x}_{P+1} | \mathrm{e}^{-i\tau H/\hbar} | \boldsymbol{x}_1 \rangle} \tag{8}$$

Inserting complete sets of states in the usual fashion yields

$$G_s(t) = \frac{\int d\boldsymbol{x}_1 \ldots d\boldsymbol{x}_{2P}\, h_a(q[\boldsymbol{x}_1]) h_b(q[\boldsymbol{x}_{P+1}])\, \Pi_{p=1}^{P} \langle \boldsymbol{x}_p | \mathrm{e}^{+i\tau^* H/P\hbar} | \boldsymbol{x}_{p+1} \rangle \Pi_{p=P+1}^{2P} \langle \boldsymbol{x}_p | \mathrm{e}^{-i\tau H/P\hbar} | \boldsymbol{x}_{p+1} \rangle}{\int d\boldsymbol{x}_1 \ldots d\boldsymbol{x}_{2P}\, \Pi_{p=1}^{P} \langle \boldsymbol{x}_p | \mathrm{e}^{+i\tau^* H/P\hbar} | \boldsymbol{x}_{p+1} \rangle \Pi_{p=p}^{2P} \langle \boldsymbol{x}_p | \mathrm{e}^{-i\tau H/P\hbar} | \boldsymbol{x}_{p+1} \rangle} \tag{9}$$

with $\boldsymbol{x}_{2P+1}^{(i)} \equiv \boldsymbol{x}_1^{(i)}$. Each $\boldsymbol{x}_p$, where $p = 1, 2, \ldots, 2P$, is a vector with $3N$ components and each $\boldsymbol{x}_p^{(i)}$ is a vector with 3 components. $2P$ is the number of ''beads'' in each path-polymer. Grouping together the real and imaginary factors of the short-time propagators, as suggested by Thirumalai and Berne [25], the normalized correlation function is written as a ratio of two integrals

$$G_s(t) = \frac{\int d\boldsymbol{x}_1 \ldots d\boldsymbol{x}_{2P}\, h_a(q[\boldsymbol{x}_1]) h_b(q[\boldsymbol{x}_{P+1}]) W(\boldsymbol{x}_1, \ldots, \boldsymbol{x}_{2P}; t) \mathscr{P}(\boldsymbol{x}_1, \ldots, \boldsymbol{x}_{2P}; t)}{\int d\boldsymbol{x}_1 \ldots d\boldsymbol{x}_{2P}\, W(\boldsymbol{x}_1, \ldots, \boldsymbol{x}_{2P}; t) \mathscr{P}(\boldsymbol{x}_1, \ldots, \boldsymbol{x}_{2P}; t)} \tag{10}$$

where

$$\mathscr{P}(x_1, \ldots, x_{2P}; t) = c(t) e^{-\beta \Phi(x_1, \ldots, x_{2P}; t)} \tag{11}$$

with

$$c(t) = \prod_{i=1}^{N} \left[\frac{m_i^2 P^2}{\pi^2 \hbar^2 (\beta^2 \hbar^2 + 4t^2)} \right]^{3P/2} \tag{12}$$

and

$$\Phi(x_1, \ldots, x_{2P}; t) = \sum_{i=1}^{N} \frac{m_i P}{(\beta^2 \hbar^2 + 4t^2)} \sum_{p=1}^{2P} \left(x_p^{(i)} - x_{p+1}^{(i)} \right)^2 + \frac{1}{2P} \sum_{p=1}^{2P} V(x_p) \tag{13}$$

$x_p^{(i)}$ is the coordinate of the p-th bead of the i-th atom, and $V(x_p)$ is the potential of the p-th copy of the system. The function $W(x_1, \ldots, x_{2P}; t)$ is a complex factor

$$W(x_1, \ldots, x_{2P}; t) = e^{-it\Omega(x_1, \ldots, x_{2P}; t)/\hbar} \tag{14}$$

with

$$\Omega(x_1, \ldots, x_{2P}, t)$$
$$= \sum_{i=1}^{N} \frac{2m_i P}{(\beta^2 \hbar^2 + 4t^2)} \sum_{p=1}^{P} \left[\left(x_p^{(i)} - x_{p+1}^{(i)} \right)^2 - \left(x_{p+P}^{(i)} - x_{p+P+1}^{(i)} \right)^2 \right] - \frac{1}{P} \sum_{p=1}^{P} \left[V(x_p) - V(x_{p+P}) \right] \tag{15}$$

(It should be noted that there were typographical errors in Refs. [24,25].) We shall write $X \equiv x_1, \ldots, x_{2P}$ as a shorthand notation. Since $\mathscr{P}(X; t)$ is real and positive, it can be used as a probability distribution and the correlation function $G_s(t)$ can be calculated as the ratio of two averages via computer simulations of a discretized Feynman path integral of $2P$-beads [26].

$$G_s(t) = \frac{\langle h_a h_b W(t) \rangle_{(t)}}{\langle W(t) \rangle_{(t)}} \tag{16}$$

where $\langle \ldots \rangle_{(t)}$ represents an average with the distribution function $\mathscr{P}(X; t)$. The function Φ can be used as the potential energy in Monte Carlo or molecular dynamics simulations of an effective system of ring polymers or necklaces of $2P$-beads [27]. Both the potential energy of the effective system and the probability distribution depend parametrically on the real time t. When $t = 0$, the normal Euclidean (imaginary) time probability distribution for a $2P$-beads discretized path integral is recovered.

Gillan and VCM stressed the importance of the equilibrium centroid density distribution in the formulation of a quantum transition rate theory [17,19,28]

$$\rho(R) = \frac{\int dX \mathscr{P}(X; 0) \delta(q_c[X] - R)}{\int dX \mathscr{P}(X; 0)} = \langle \delta(q_c[X] - R) \rangle_{(0)} \tag{17}$$

where $q_c[X]$ is the centroid of the reaction coordinate function,

$$q_c[X] = \frac{1}{2P} \sum_{p=1}^{2P} q[x_p] \tag{18}$$

The centroid density $\rho(R)$ is independent of time and straightforward to compute. The value of $\rho(R)$ dominates the magnitude of the rate because it depends exponentially on the free energy of the system as a function of R, i.e., $\mathscr{W}(R) = \mathscr{W}(R_0) - k_B T \ln[\rho(R)/\rho(R_0)]$ is the centroid potential of mean force [17,19]. If the integrand of

the normalized side–side correlation function is written so as to expose $\rho(R)$, the calculation of the rate constant can be facilitated. In addition, by separating the purely statistical factor $\rho(R)$ one highlights the influence of dynamical factors. $\rho(R)$ determines the magnitude of the correlation function.

One can introduce the equilibrium centroid density into the above equation for $G_s(t)$ by multiplying by $\delta(q_c[X] - R)$ and integrating over R, yielding

$$G_s(t) = \int_{-\infty}^{\infty} dR \, \frac{\int dX \, \delta(q_c[X] - R) h_a(q[x_1]) h_b(q[x_{P+1}]) W(X;t) \mathscr{P}(X;t)}{\int dX \, W(X;t) \mathscr{P}(X;t)} = \int_{-\infty}^{\infty} dR \, g_s(t;R) \rho(R)$$

(19)

where

$$g_s(t;R) = \frac{\langle e^{-\beta \Delta \Phi(t)} \rangle_{(0,R)} \langle h_a h_b W(t) \rangle_{(t,R)}}{\int_{-\infty}^{\infty} dR' \, \rho(R') \langle e^{-\beta \Delta \Phi(t)} \rangle_{(0,R')} \langle W(t) \rangle_{(t,R')}}$$

(20)

In Eq. (20), the notation $\langle \ldots \rangle_{(t,R)}$ represents an average performed with the probability distribution $\mathscr{P}(X;t)$ with the centroid reaction coordinate fixed at R. In particular,

$$\langle e^{\beta \Delta \Phi(t)} \rangle_{(0,R)} = \frac{\int dX \, e^{\beta \Delta \Phi(t)} \delta(q_c[X] - R) \mathscr{P}(X;0)}{\int dX \, \delta(q_c[X] - R) \mathscr{P}(X;0)}$$

(21)

where $\Delta \Phi(t) = \Phi(X;t) - \Phi(X;0)$, is the potential energy difference of the effective system for two different parametric values of the time t. Alternatively one can write

$$g_s(t;R) = \left\langle h_a h_b W(t) \frac{c(t)}{c(0)} e^{-\beta \Delta \Phi(t)} \right\rangle_{(0,R)}$$

(22)

where the identity $\int dX \, W(X;t) \mathscr{P}(X;t) = \int dX \, \mathscr{P}(X;0)$ has been used. Other formally equivalent formulations are possible. Since only $g_s(t;R)$ depends on the time t, the rate constant is easily calculated from the time-derivative of the correlation function

$$k = \frac{Q}{Q_a} \lim_{t \to \tau_m} \int_{-\infty}^{\infty} dR \, \dot{g}_s(t;R) \rho(R)$$

(23)

or

$$k = \lim_{t \to \tau_m} \frac{\int_{-\infty}^{\infty} dR \, \rho(R) \dot{g}_s(t;R)}{\int_{-\infty}^{\infty} dR \, \rho(R) h_a(R)}$$

(24)

or lastly, the rate may be expressed in terms of the centroid potential of mean force,

$$k = \lim_{t \to \tau_m} \frac{\int_{-\infty}^{\infty} dR \, e^{-\beta \mathscr{W}(R)} \dot{g}_s(t;R)}{\int_{-\infty}^{\infty} dR \, e^{-\beta \mathscr{W}(R)} h_a(R)}$$

(25)

Eqs. (16), (20) and (25) are the principal results of this letter.

The present formulation is directly amenable to computer simulations because the rate constant is expressed only in terms of quantities which are configurational averages with real positive probability distribution functions. All averages are calculated using the probability distribution function of the effective system, $\mathscr{P}(X;t)$, which depends parametrically on the real time t. The calculation of the rate requires the time-derivative of $g_s(t;R)$. Time appears in two different ways in our equation for $g_s(t;R)$: an average is computed with a probability distribution that depends on time and the quantity which is averaged also depends on time. If we wished to compute $g_s(t;R)$ at a only single value of t, say $t = t_k$, we would use the probability distribution at that value of t, $\mathscr{P}(X;t_k)$ and average $h_a h_b W(t_k)$. However, we need to obtain $g_s(t;R)$ as a function of time. We can use Monte Carlo configurations generated from $\mathscr{P}(X;t_k)$ to compute the average at t_k, but we can also use the same configurations to compute averages at other times. Because there is a family of probability distributions corresponding to different values of the time t, it is desirable to use simulations performed with several members of the family to extract the best possible averages at many values of time. This situation is analogous to the well-known problem of free energy perturbation [29] and umbrella sampling [30] in simulations of classical systems. For such calculations, powerful methods have been developed to calculate averages from a family of ensembles depending parametrically on an external parameter (here the time ''t''). In particular, the weighted histogram analysis method (WHAM) allows one to combine information from simulations generated in different ensembles to obtain optimal averages [31,32]. Assume that a set of m simulations has been generated with different values of time $t = \{t_1, t_2, \ldots, t_m\}$. For the k-th simulation, n_k configurations are available. Let $X_{i,k}$ be the i-th configuration from the simulation generated with t_k. Using all the available information, it is possible to obtain the best estimate for the average of an observable $\langle A(t_k)\rangle_{(t_k)}$ in the t_k-ensemble,

$$\langle A(t_k)\rangle_{(t_k)} = \sum_{i=1}^{m} \sum_{l=1}^{n_i} \frac{A(X_{i,l};t_k)e^{-\beta[\Delta\Phi(X_{i,l};t_k)-f_k]}}{\sum_{j=1}^{m} n_j e^{-\beta[\Delta\Phi(X_{i,l};t_j)-f_j]}} \tag{26}$$

where $\Phi(X_{i,l};t_k)$ is the energy calculated with t_k using the i-th configuration of the t_l simulation. The coefficients f_k are obtained self-consistently from the equation

$$e^{-\beta f_k} = \sum_{i=1}^{m} \sum_{l=1}^{n_i} \frac{e^{-\beta\Delta\Phi(X_{i,l};t_k)}}{\sum_{j=1}^{m} n_j e^{-\beta[\Delta\Phi(X_{i,l};t_j)-f_j]}} \tag{27}$$

which can be solved iteratively. It should be stressed that, because the rate constant is expressed as averages from a probability distribution, one can explicitly compute the time-derivative of any function of time $A(t)$,

$$\frac{d}{dt}\langle A(t)\rangle_{(t)} = \langle \partial A(t)/\partial t\rangle_{(t)} - \beta\big[\langle A(t)\,\partial\Delta\Phi(t)/\partial t\rangle_{(t)} - \langle A(t)\rangle_{(t)}\langle \partial\Delta\Phi(t)/\partial t\rangle_{(t)}\big] \tag{28}$$

3. Discussion

3.1. Relation to TST

The equation we present for the thermal rate constant is exact. It is exact because it follows from the MST formulation without making approximations. Of course, other rigorous expressions have been proposed previously. The key advantage of the present formulation is that it is amenable to Monte Carlo simulations. Calculations are discussed in the next subsection but it is also of interest to demonstrate explicitly the relation

between our equation and classical transition state theory (TST) and the ''quantum transition state theory'' formula proposed by Voth, Chandler, and Miller (VCM) [19].

The VCM equation can be inferred from our equation in two steps: (i) isolate $\int_{-\infty}^{\infty} dR\, \dot{g}_s(t;R)$, and (ii) use a TST approximation to evaluate it. Step (i) is motivated by the fact that the time-derivative, $\dot{g}_s(t;R)$, is a function which is expected to be sharply peaked at the transition state $R^\dagger$ (see Fig. 2). Therefore, assuming that the function $\rho(R)$ varies smoothly,

$$k \approx \lim_{t \to \tau_m} \frac{Q}{Q_a}\rho(R^\dagger)\int_{-\infty}^{\infty} dR\, \dot{g}_s(t;R) \tag{29}$$

All dynamical effects are included in the correlation function $\dot{g}_s(t;R)$. One way to accomplish step (ii) is to replace the dynamical factor in Eq. (29) by the corresponding free particle dynamical factor, i.e., one assumes the system reacts (as a free particle would) if the momentum along the reaction coordinate (towards products) is positive [5,23]. In the same spirit, it is reasonable to approximate k by introducing a free-particle dynamical factor $\dot{g}_s^{\mathrm{fp}}(t;R)$ [17,19]

$$k \approx \frac{Q}{Q_a}\rho(R^\dagger)\lim_{t \to \tau_m}\int_{-\infty}^{\infty} dR\, \dot{g}_s^{\mathrm{fp}}(t;R) \tag{30}$$

For a free particle we can put $\tau_m = \infty$. To evaluate $\int_{-\infty}^{\infty} dR\, \dot{g}_s^{\mathrm{fp}}(t;R)$ we use the fact that,

$$\int_{-\infty}^{\infty} dR\, \dot{g}_s^{\mathrm{fp}}(t;R) = \frac{\dot{C}_s^{\mathrm{fp}}(t)}{Q^{\mathrm{fp}}(R^\dagger)} \tag{31}$$

which follows directly from Eqs. (2), (20) and (16). The quantity $Q^{\mathrm{fp}}(R^\dagger) = \sqrt{2\pi m k_B T}/h$ is the partition function of the system constrained at the transition state, and

$$\dot{C}_s^{\mathrm{fp}}(t) = \frac{k_B T}{h} \frac{t}{\sqrt{t^2 + (\beta\hbar/2)^2}} \tag{32}$$

Therefore,

$$\int_{-\infty}^{\infty} dR\, \dot{g}_s^{\mathrm{fp}}(t;R) = \frac{1}{\sqrt{2\pi m\beta}} \frac{t}{\sqrt{t^2 + (\beta\hbar/2)^2}} \tag{33}$$

The centroid-TST equation of VCM [19] is recovered by taking the limit as $t \to \infty$ and substituting this result into Eq. (30),

$$k_{\mathrm{VCM}} = \frac{Q}{Q_a}\rho(R^\dagger)\frac{1}{\sqrt{2\pi m\beta}} \tag{34}$$

Equivalently, the VCM rate constant may be written in an Arrhenius form [19]

$$k_{\mathrm{VCM}} = \frac{1}{Q_a}\frac{k_B T}{h}\mathrm{e}^{-\beta\mathscr{W}(R^\dagger)} \tag{35}$$

by defining $\mathscr{W}(R^\dagger) = -k_B T \ln[Q(R^\dagger)/Q^{\mathrm{fp}}(R^\dagger)]$. In the classical limit, one recovers the standard TST equation for the rate constant,

$$k_{\mathrm{TST}} = \frac{1}{\sqrt{2\pi m\beta}}\frac{Q_{\mathrm{cl}}^{fp}(R^\dagger)}{Q_{\mathrm{cl},a}} \tag{36}$$

because $Q_{\mathrm{cl}}^{fp}(R^\dagger)$ is the classical partition function when R is constrained at $R^\dagger$, and $Q_{\mathrm{cl},a}$ is the classical

partition function for region a. From the point of view of path integral simulations, the polymer necklace for atom i shrinks to a single point and $\mathscr{W}(R^{\dagger})$ approaches the classical potential of mean force at $R^{\dagger}$.

The potential of mean force at the transition state is the dominant factor determining the magnitude of the rate and it is generally expected that the dynamical factor should play a less important role. VCM exploited this observation by calculating the potential of mean force at the transition state exactly but approximating the dynamical factor with results from simple models which can be solved analytically [19]. In fact, using their approach it was *necessary* to approximate the dynamical factor because it was expressed as the Kubo transform of a flux–flux correlation function involving real-time propagators which are not easily amenable to computer simulations. It should be emphasized that, using our equation for the rate constant, it is possible, not only in principle but also in practice, to calculate $\dot{g}_s(t;R)$ for a complex system from a computer simulation. Thus, it is not necessary to use results from simple models (e.g., free particle, parabolic barrier) to evaluate the dynamical factor.

3.2. Computational example

Our equation for k will be useful if one is able to calculate the averages in Eq. (20) or Eq. (22) with path integral simulations. To illustrate the present formulation, a free proton at $T = 300$ K in one dimension is considered. Although this is a very simple system, it is adequate to illustrate the non-trivial computation of $\dot{g}_s(R;t)$ with computer simulations. Furthermore, it should be stressed that the computational difficulties are mostly due to the oscillatory nature of $W(t)$ arising from the real-time propagators and may not depend sensitively on the potential.
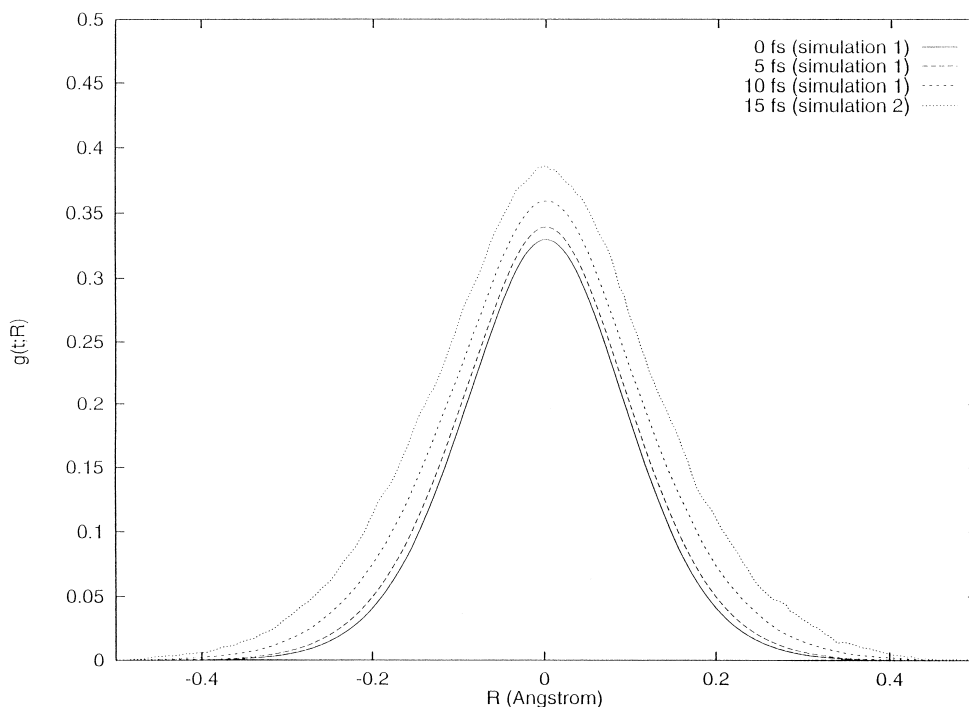

Fig. 1. The correlation function $g_s(t;R)$ calculated for a free particle with the centroid constrained at R using Metropolis Monte Carlo and WHAM. The correlation function is shown for $t = 0$, 5, 10 and 15 fs. Simulation 1 is a calculation with 10^5 configurations and simulation 2 is with 5×10^5 configurations.

Two million configurations were generated using Monte Carlo path integral simulations for $t = 0, 5, 10, 15,$ and 20 fs with random moves of 0.1 Å (simulation 1). The discretized paths were represented by a necklace of 20 beads ($P = 10$). A simple Metropolis importance sampling algorithm with symmetric random moves was used [33,34]. The average acceptance rates for the five simulations were 33, 37, 45, 54 and 62%. The acceptance ratio increases with t due to the increasing extension of the paths. 10^5 configurations were written on disk and kept for the WHAM analysis. A separate simulation with 5×10^5 configurations was generated to obtain a more accurate estimate for $t = 15$ fs (simulation 2).

In Fig. 1 we show the left-right side–side correlation function $g_s(t;R)$ for $t = 0$, 5, 10, and 15 fs as a function of the centroid position R. We calculate $g_s(t;R)$ at 300 equally spaced points between -0.75 and $+0.75$ Å. The $g_s(t;R)$ functions have Gaussian-like shapes with maxima at the dividing surface and full width at half maxima (FWHM) of about 0.2 Å, which is close to half the thermal de Broglie wavelength of a proton at $T = 300$ K. With increasing time t both the FWHM and height of the left-right side–side correlation function plots increase. The time-derivative of the left-right side–side correlation function, $\dot{g}_s(t;R)$, is shown for $t = 5$, 10 and 15 fs in Fig. 2, as a function of the centroid position. We calculate the derivative with a two-point formula and a step size of 1.0 fs. The time-derivative plots are doubly peaked functions (with one peak on the reactant side and one peak on the product side of the dividing surface) with a shallow well centred on the dividing surface, $R = 0$. The overall width and height of the curves increase with t. The area under the $\dot{g}_s(t;R)$ curve should increase with t because it is equal to the value on the right hand side of Eq. (33). Fig. 3 illustrates this point. In Fig. 3 the integral over the centroid position R of $\dot{g}_s(t;R)$, is shown. We plot the results from our numerical simulation (as points) with the analytical result as a solid line. The integral is obtained with the trapezoid method and a step size of 0.005 Å. For the 15 fs case we verified that the trapezoid and Simpson's rule methods give equivalent results. The integral of $\dot{g}_s(t;R)$ in Eq. (33) yields an average reactive velocity. For
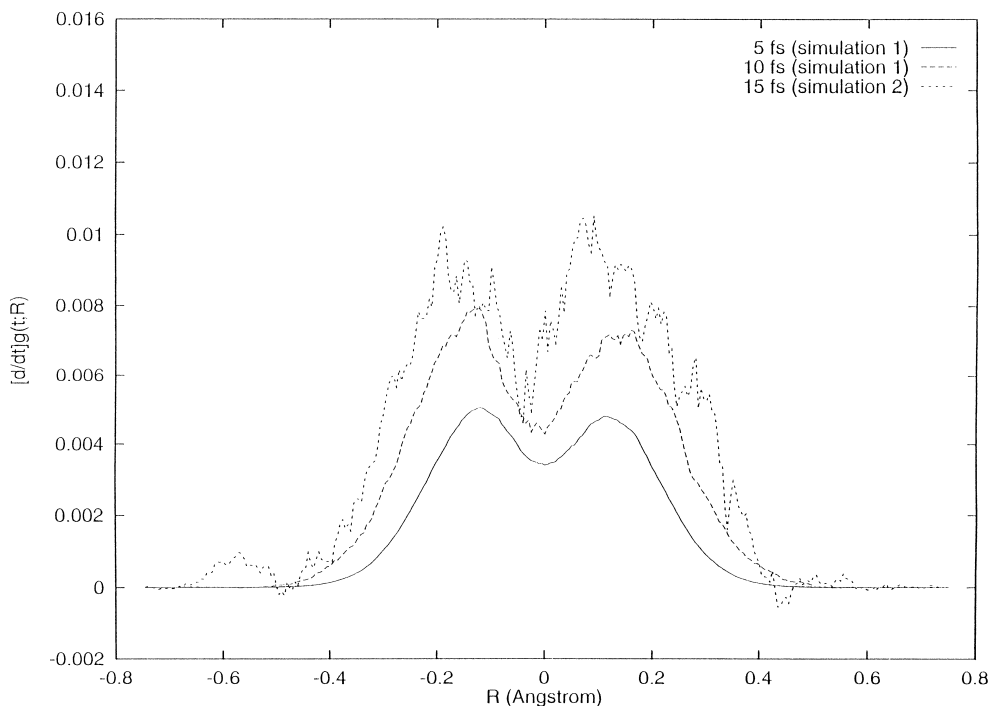

Fig. 2. The correlation function $\dot{g}_s(t;R)$ calculated from the time derivative of $g_s(t;R)$ shown in Fig. 1. The time derivative was calculated with finite differences using a time increment of 1 fs using WHAM.
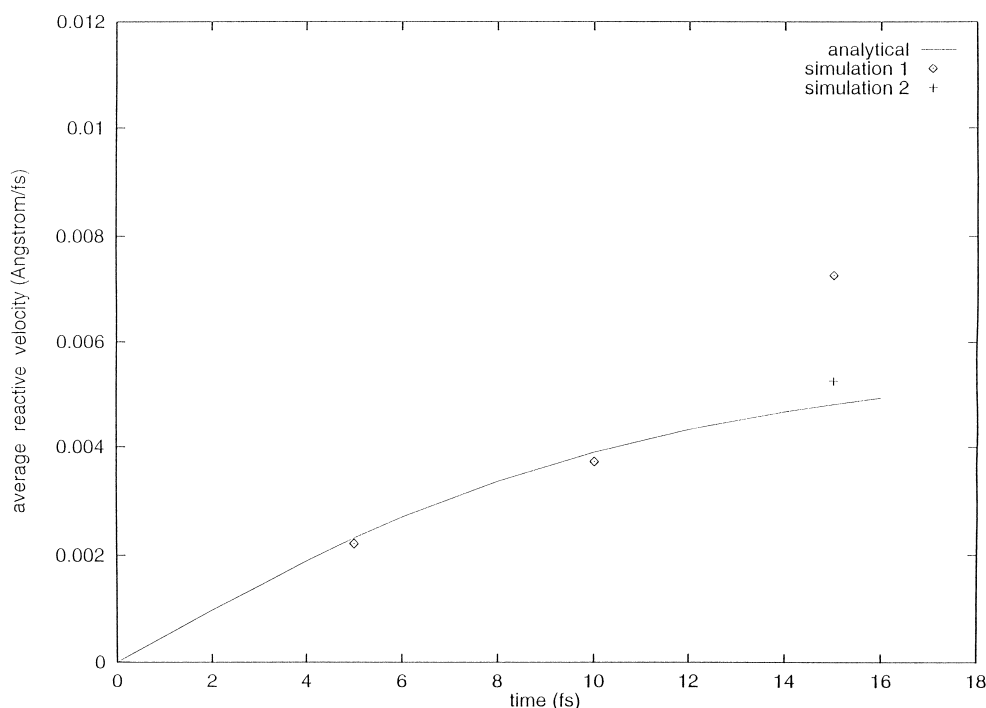
Fig. 3. Reactive velocity. The results from numerical integration of $\dot{g}_s(t;R)$ and the exact analytical answer (solid line) are shown. For a free particle, the plateau value is equal to $1/\sqrt{2\pi\beta m} = 0.0063$ Å/fs. The results shown with diamonds are obtained from simulation 1 (with 10^5 configurations) and result indicated with a "+" is obtained from simulation 2 (with 5×10^5 configurations).

a free proton, the limiting value is 0.0063 Å/fs. As shown by the two calculations at $t = 15$ fs, the accuracy of the calculated average reactive velocity decreases at times approaching $\beta\hbar$. However, according to classical simulations of realistic models [35] it is expected that the reactive flux will reach a plateau in 10 to 15 fs for many proton transfer reactions. Thus, although the calculation of $\dot{g}_s(t;R)$ by computer simulations is difficult, it appears to be possible in the required time range.

The slow convergence is due to the behavior of the function $W(t)$. The average $\langle W(t) \rangle_{(t)}$ decreases rapidly as a function of t, changing from about 0.52 for $t = 5$fs, to 0.002 for $t = 20$ fs. This indicates, not surprisingly, that $W(t)$ oscillates very rapidly as t increases. The oscillation of $W(t) = \exp[-it\Omega/\hbar]$ is indicative of extensive phase-averaging at longer times. This suggests that sampling biased towards regions of the configurational space in which the phase $\Omega(X,t)$ is stationary may provide an effective computational strategy for improved convergence [22].

4. Conclusion

We have developed a rigorous and practical method based on Feynman path integrals for calculating rate constants for quantum systems. Eqs. (16), (20) and (24) are the principal results of this letter. The fundamental elements of our formulation are:
· The quantum mechanical expression for the thermal rate constant in terms of a side–side correlation function developed by Miller, Schwartz and Tromp (MST) [11];
· The method of Thirumalai and Berne [24] to calculate real-time symmetrized correlation functions from Feynman path integral computer simulations;

- The concept of the centroid of a thermal path (Feynman [20], Gillan [17], Voth et al. [19]);
- Use of statistical mechanical free energy perturbation methods [29], biased sampling [30], and the Weighted Histogram Analysis Method (WHAM) [31,32] to extract information from simulations of paths with different values of t.

An important element of the present formulation is the MST side–side correlation function. In principle one could calculate the rate constant from the side–side, flux–side or flux–flux correlation function; the rate constant is related to the time-derivative of the side–side correlation function, the plateau value of the flux–side correlation function, and the time-integral of the flux–flux correlation function [11]. The three formulations are formally and rigorously equivalent. However, if one uses a path integral formulation it is *much* easier to *first* calculate the side–side correlation function, and and *then* compute the time-derivative. The side–side correlation function is expressed in terms of population operators and the trace with the density matrix is easily calculated. This obviates the difficulties in calculating a trace involving matrix elements of the flux operator. In the present formulation we must differentiate the side–side correlation function to obtain the rate constant, but as shown by the present work, it is not difficult to differentiate *after* computing the trace.

The theory was illustrated for a free particle, however application to other systems should not be fundamentally different. Although the present formulation involves only real and positive distribution probability functions, it is nevertheless difficult to obtain accurate averages for t close to or larger than $\beta\hbar$. However, previous simulations based on realistic models of proton transfer reactions showed that, for some simple and direct reactions, the classical reactive flux reaches a plateau value in 10 to 15 fs [35]. Thus, although the rigorous quantum mechanical calculation of a transition rate constant with computer simulations is difficult, it appears to be possible. To describe less direct reactions requiring evaluation of $\dot{g}_s(t;R)$ for $t \sim 25$–50 fs it will be important to develop more effective sampling methods. The powerful statistical mechanical methods of biased sampling and free energy perturbations will be of great utility for improving the convergence of these calculations. Further work is currently in progress in these directions.

Acknowledgements

References

[1] M. Karplus, In C. Schlier, editor, Molecular Beams and Reaction Kinetics Academic Press, London, (1970).
[2] D. Chandler, J. Chem. Phys. 68 (1978) 2959.
[3] P. Hänggi, P. Talkner, M. Borkovec, Rev. Mod. Phys. 62 (1990) 251.
[4] B.J. Berne, In J.U. Brackbill, B.I. Cohen, editors, Multiple Time Scales pages 419–436. Academic Press, New York, (1985).
[5] W.H. Miller, Acc. Chem. Res. 9 (1976) 306.
[6] J.C. Keck, Adv. Chem. Phys. 13 (1976) 85.
[7] S.H. Northrup, J.T. Hynes, J. Chem. Phys. 73 (1980) 2700.
[8] J.B. Anderson, J. Chem. Phys. 58 (1973) 4684.
[9] T. Yamamoto, J. Chem. Phys. 33 (1960) 281.
[10] W.H. Miller, J. Chem. Phys. 61 (1974) 1823.
[11] W.H. Miller, S.D. Schwartz, J.W. Tromp, J. Chem. Phys. 79 (1983) 4889.
[12] U. Manthe, W.H. Miller, J. Chem. Phys. 99 (1993) 3411.
[13] U. Manthe, J. Chem. Phys. 102 (1995) 9205.
[14] T.J. Park, J.C. Light, J. Chem. Phys. 88 (1988) 4897.
[15] T. Seideman, W.H. Miller, J. Chem. Phys. 97 (1992) 2499.
[16] S.M. Miller, T. Carrington Jr, Chem. Phys. Lett. 267 (1997) 417.

[17] M.J. Gillan, J. Phys. C 20 (1987) 3621.
[18] G.A. Voth, D. Chandler, W.H. Miller, J. Chem. Phys. 91 (1989) 7749.
[19] G.A. Voth, J. Phys. Chem. 97 (1993) 8365.
[20] R.P. Feynman, A.R. Hibbs, Quantum Mechanics and Path Integrals McGraw-Hill, New York, (1965).
[21] L.S. Schulman, Techniques and Applications of Path Integration, John Wiley and Sons, New York, (1981).
[22] N. Makri, Comp. Phys. Comm. 63 (1991) 389.
[23] D. Chandler, Introduction to Modern Statistical Mechanics Oxford University Press, Oxford, (1987).
[24] D. Thirumalai, B.J. Berne, J. Chem. Phys. 81 (1984) 2512.
[25] B.J. Berne, J. Stat. Phys. 43 (1986) 911.
[26] D. Thirumalai, B.J. Berne, Comp. Phys. Comm. 63 (1991) 415.
[27] D. Chandler, P.G. Wolynes, J. Chem. Phys. 74 (1981) 4078.
[28] G.A. Voth, Adv. Chem. Phys. 93 (1996) 135.
[29] R.W. Zwanzig, J. Chem. Phys. 22 (1954) 1420.
[30] G.M. Torrie, J.P. Valleau, Chem. Phys. Lett. 28 (1974) 578.
[31] A.M. Ferrenberg, R.H. Swendsen, Phys. Rev. Lett. 63 (1989) 1195.
[32] S. Kumar, D. Bouzida, R.H. Swendsen, P.A. Kollman, J.M. Rosenberg, J. Comp. Chem. 13 (1992) 1011.
[33] N. Metropolis, A.W. Rosenbuth, M.N. Rosenbuth, A.H. Teller, E. Teller, J. Chem. Phys. 21 (1953) 1087.
[34] M.P. Allen, D.J. Tildesley, Computer Simulations of Liquids, Clarendon Press, Oxford, (1987).
[35] K. Hinsen, B. Roux, J. Chem. Phys. 106 (1997) 3567.